Webology (ISSN: 1735-188X)
Volume 18, Number 6, 2021

Stability Lobe Diagram For Optimization Of Turning Chatter In Machining

[1]Akshat Singh Jhala , [2]Dr. Manish Pokharna

[1]Research Scholar, Faculty of Engineering, Pacific Academy of Higher Education and Research University Udaipur, Rajasthan.

[2]Professor, Pacific Academy of Higher Education and Research University Udaipur, Rajasthan.

Abstract

This paper investigates some fundamentals of vibration in cutting tools. It has been reported that chatter phenomenon may be the result of both self-induced and forced vibration where self-induced vibration is considered to be a function of the cutting properties of the metal and the sharpness of the tool, while the forced vibration depends on the interference of the tool with the surface cut during previous revolutions. There are some speed, frequency, and sharpness restrictions in place, with vibration being infrequently seen at low cutting speeds, high tool frequencies, or with recently lapped tools. Self-excited regenerative vibration or chatter limits the primary requirements like productivity, surface finish and dimensional accuracy of high-speed machining. The most dependable strategy for reducing and eliminating chatter is to choose the machining settings using a stability lobe diagram. Knowing particular cutting force coefficients and tool point frequency response functions (FRFs) is often required to produce stability lobe diagrams. Stability lobe diagrams' stable zones are greatly impacted by improper tool point FRF use. Plotting the stability limits and chatter frequency results in the stability lobe diagram for the developed theoretical model. The Transfer Function (TF) or Frequency Response Function (FRF) of the machine tool-tool holder-tool system gives the system the essential data (dynamic characteristics). High quality microphone to record the vibration was used to track the chatter reaction. The natural frequency, modal stiffness, and damping coefficient of the tool vibration, which are typically obtained by the frequency response function (FRF) of the system, have been calculated in order to create the stability lobe diagram of the tool vibration. The project envisase to find solution to improve the material removal rate without compromising the surface fisnish and machining tolerance of the workpiece, which compeled to consider the prediction model of MRR and chatter severity. These two factors have been developed and analysed to obtain optimal stablerange of turning parameters with lower chatter and improved material removal rate so that quality ahd accuracy could be mainained with high productivity.

Keywords: Stability lobe diagram, SLD, Chatter, vibration, turning, CNC lathe, OMA, Operational model analysis, regenerative vibration, self-excited vibration.

Introduction

Machining process are subject to dynamic effects due to transient or forced vibrations, and dynamic mechanisms inherent to the process like regeneration, which results in high amplitude oscillations, instability and poor quality. Depending on the sources of energy, tool vibrations are engerally chategorized as forced vibrations and self-excited vibrations. Force vibrations are associated with disturbing periodics forces resulting from the unbalanced of rotating parts, from the intermittent engagement of workpiece with multi-flute cutters or from errors of accuracy on some driving components.[1] Dynamically unstable system corresponds to unstable vibration between the workpiece and tool and, usually known as self- excited vibrations or chatter, which occur under certain conditions generally associated with the increase of the material removal rate, and these are enerziged by the cutting process itself.

In the turning process there are three types of mechanical virbrations are detected due to lack of dymnamic stiffness or rigidity of the machine tool system consisteing of workpiece, cutting tools, toll holder and machine tools. The process was first examined and explained by Tobia[2]. Three types of vibration are, Free virbration, forced vibration and self-excited vibration. Free vibration normally induced by shock, forced vibration generated due to unbalanced effects in machine tool assembalies such as gears, bearings, spindles, etc., these two vibrations can easiliy be detected and appropriate measures can be taken to rectify or suppress the generated vibration. Third vibration is self-excited vibrations which has been still not fully understood till now because of complexity involved in it and are considered to be hazardous for quality production and accuracy in any machining process including turning operations. Self-excited vibrations are generally suggested to be of two type, first primary chatter and second, secondary chatter[3]. Primary chatter is generated due to friction between thermo-mechanical effects, tool-workpiece or by mode coupling effect, while secondary chatter is generated by the regeneration of wavy surface or roughness on the workpice. Regenrative chatter is considered to be more destructive in nature, because it decreases the quality and accuracy of the product. Various methods has been adopted to find the solution by scholars in this direction, such as by predicting chatter occurances earlier or detecting it as soon as it occurs, active and passive control strategies has been tried by researchers to control the chatter.

Chatter can occur in different metal removal processes and has several negative effects such as Poor surface quality, unacceptable inaccuracy, excessive noise, dispropostionate tiil wear, nachine tool damage, reduced material removal rate, increased costs in terms of production time, waste of materials, waste of energy, environmental imact in terms of mateials and energy and cost of recycling, reprocessing or dumping non-valid final parts to recycling points. It has been observed that frictional chatter, thermo-mechanical chatter and mode coupling chatter and regenerative chatter can be distinguished depending on the self-excittation mechanism that cause the vibration[4]. When friction is applied to the clearing face, it stimulates vibration in the direction of the cutting force Fc and limits it in the direction of the thrust force Ft[5]. The temperature and strain rate in the plastic deformation zone cause thermo-mechanical chatter[6]. If vibration in the thrust force direction causes vibration in the cutting force direction, and vice versa, then there is mode coupling chatter[7],[8],[9]. This causes simultaneous vibrations in the directions of the thrust and cutting forces. Physically, it is brought on by a variety of factors, including friction on the clearing and rake surfaces, fluctuation in chip thickness, oscillations in shear angle, and regeneration effect[10]. Self-excited vibration most frequently takes the form of regenerative chatter. Since most metal cutting operations involve overlapping cuts, which

can be a source of vibration amplification, it might happen frequently. A wavy surface is left behind by the cutter vibrations and the following tooth in the cutting sequence creates a new wavy surface when milling this surface. Due to the phase difference between the wave left by the current teeth and the wave left by the preceding teeth (in turning process, this is the surface left after the previous revolution), the chip thickness and, consequently, the force on the cutting tool varies[10],[11],[12].

Chatter prediction can bee visualized through stability lobe diagram (SLD) where the border between a stable cut, i.e. where no chatter exists and an unstable cut, i.e. where chatter can be detected. The effect can be visualsied in terms of the axial depth-cut as a function of the spindle speed, which can find the specific combination of machining parameters that result in the maximum chatter-free material removal rate (MRR).[13]

Previous works investigated

Taylor[14], who conducted in-depth research on metalcutting processes as early as the 1800s, was the first to identify chatter as a productivity barrier in machining. Chatter is the "most obscure and delicate of all problems facing the machinist," according to a 3/4 power law cutting force model that was developed. For lathes and other machines, Arnold[15] looked at a variety of influences that a tool is subjected to while cutting both analytically and empirically. He also discussed the mechanisms creating chatter and recommended cutting forces as a function of speed.

It was demonstrated that the most crucial attribute of chatter vibration is that the forces that create and sustain it are generated within the vibratory process (dynamic cutting process), rather than being driven by external periodic forces. Chatter is brought on by instability in the cutting operations, which Tobias and Fishwick[16] and Tlusty and Polacek[17] were the first to recognize. It was found that vibration-induced modulated chip thickness impacts cutting forces dynamically, which in turn causes vibration amplitudes to grow and result in regenerative chatter. Additionally, it was found that the cutting process stability's primary process parameter was the depth of cut.

For orthogonal cutting, Tlusty and Polacek[18] presented a stability condition in which stability limits can be calculated based on the system dynamics. Analytically, they demonstrated that for cuts deeper than the stability limit, the magnitude of the dynamic forces and oscillations increases, leading to instability and resulting chatter vibrations. The solution can only be used to a one-dimensional process because cutting forces and structural dynamics were only resolved in one direction, i.e., the chip thickness direction. Tobias[19] and Meritt[20] researched the modeling of regeneration chatter's dynamic response, structural characteristics, and stability limit issues. These investigations are only applicable to orthogonal cutting, when the system dynamics, chip thickness, and cutting force direction are constant across time.

Much research has been done on improving the material removal rate (MRR) and surface quality by setting optimal machining parameters and controlling machine tool chatter. Regenerative chatter theory [21],[22], [23], [24] presents a relationship between spindle speed and the critical chip width or depth of cut. The theory produces a stability lobe diagram (SLD) and makes it possible to achieve the highest applicable MRR for a machining process. In recent

period, majority of researches have focused on topics such as multimode chattering, variations of machine tools and cutting tools, numerical modeling, and instrumental measurements. However, a thorough discussion of chatter theory and equations, along with improvement to techniques for creating the stability lobe diagram, are equally important.

The boundary between a chatter-free stable cut and an unstable cut with chatter, that can be exihibited in stability lobe diagram (SLD), shows relationship between the two cutting parameters. Stability lobe diagram has been used by several researchers to perform stability analysis, where a mathematical delay differential equation to plot the stability lobe diagrams has been used. Researchers have suggested that stability conditions can be predicted by drawing stability chart w.r.t. cutting parameters viz. cutting speed and depth of cut[25]. It has been aslo observed that material removal rate can be improved by limiting self-excited chatter. As illustrated in Figure 1, stability in turning using stability lobe diagram (SLD) has been predicted by Das and Tobias[26], where researchers have suggested that SLD offers boundary between stable and unstable cut. The stability analysis of machining using stability lobe diagram has also been presented by Tlusty[27]. The stability lobe diagram from the cutting tool sysem, the workpiece and the machine tooling under certain conditions is constantly changing, which makes it very difficult to obtain forecasts and correct paramenters in order to confirm stable machining. It has been reported that the influence of feed rate on chatter cannot be ascertained using SLD. Since feed rate is an important cutting parameter governing chatter, its why it will be not wise move to ignore it beause feed rate on turning stability has adverse effects when overlooked by the previous researches. Some researchers relate the stability of the machining with the vibration of the chatter using surface roughness[28]. Chatter prevents the necessary surface finishes feom being produced and reduces the life of tools and machinery parts, which is essential to study to find effective solution for accuracy and result.

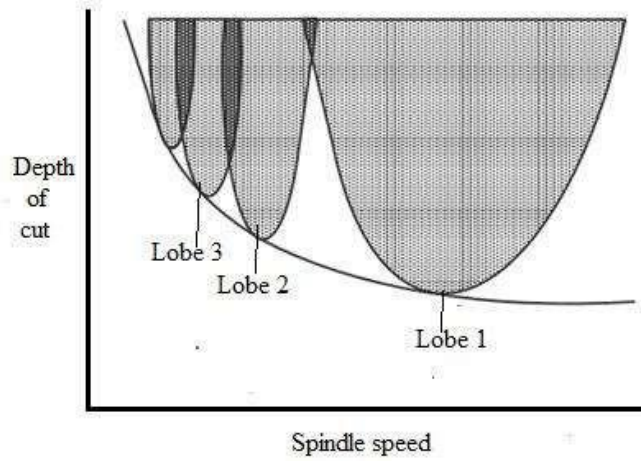

Figure 1: Stability lobes with instability in shaded portions[29]

Several scholars have used the stability lobe diagram to illustrate the chatter analysis. The stability lobe diagram can also be plotted using the established model[30]. According to Meritt's[31] presentation of stability requirements using stability charts for self-excited vibrations, chatter can be predicted in terms of the input cutting parameters, namely cutting speed and depth of cut.

Analytical methods for chatter prediction have been investigated by several scholars. Following a study of these important studies, it has been concluded that the sDoF model can forecast the beginning of chatter. Models of higher order are redundant, because numerically resolving analytical modeling techniques can be time-consuming and challenging, these relationships have been used to create simulated signals and then analyze them using stability lobe diagrams. SLD provides a stability chart that makes it simple to forecast unstable, stable, and transitional points in relation to depth of cut and cutting speed. The disadvantage of SLD is that it cannot foresee how feed rate will affect stability. Furthermore, since it is a crucial cutting parameter affecting the rate of material removal, the impact of this cutting parameter cannot be disregarded.

Mechanism and experiment

In unmanned turning operation, automatic detection of regenerative chatter play very crucial role in most of the manufacuting industries in order to avoid detrimental effects on surface integrity and damage on the workpiece or machine tools caused by satastrophic tool failure resulting from large amplitude vibrations. Experimental techniques provide way to predict the stability condition in offline mode and detecting chatter onset in online mode. Analytical SLD could be half way mark in detecting the chatter completely which can be done with actual cutting tests. Theoretical and practical both method should be applied to reach the goal and this identification of chatter onset is possible using tool condition monitioring (TCM) techniques. The condition monitoring depends upon the type of machine tool as suggested by Siddhpura et. al.[30]. Tool monitoring can be performed through force, vibration and acoustic signals which paly very important role in monitoring process. Various sensors can play crucial role in verification and detection of predicted chatter stability which can measure force, displacement, velocity, acceleration, acoustic signals generated from a machining process, that can be obtained through different appropriate sensors application. Traditional signal processing techniques such as time-domain, frequency domain and teme-frequency domain analysis are generally explored.

Eexperimental model analysis has used MTAB XLTURN CNC lathe. The selected CNC is a 2-axis benchtop slant bed lathe with 8 station programmable turret. Machine has Fanuc or Siemens emulated control system or MTAB Industrial Control and can be integrated with modular automation components to create Smart Factory Automation Systems (FMS, CIM), sutaible for prototyping. It gives 150-3000 rpm spindle speed, max turning diameter 32 mm, max. turning length 120 mm and have 8 stations carbide insert TTSO4 tool has been used in turning process. A1-6061-T6 has been selected for the work. Aluminum 6061-T6 is commonly-used aluminum alloy in manufacturing sectors like aerospace, defense and automobile industries due to its good mechanical properties, good weldability and high corrosion resistance. Machining is important part in these manufacturing chains; hence material has been selected keeping in view its wide applicability. Microphone of 50-15,000 HZ frequency response of AHUJA AGN-500 has been used for recording.

Machining parameters considered for the experiment has been summurised in Table 1.

Table 1: Experimental cutting condition Input parameters and their levels

S. No.	Experimental Parameters	Experimental levels		
		P1	P2	P3
1.	h_0	0.2	0.3	0.4
2.	Ω	1000	1500	2000
3.	f	30	35	40
4.	D	36.50	35.00	33.50

In the Table 2 given parameters are –

P1 – First Level

P2 – Second Level

P3 – Third Level

h_0 - depth of cut (mm)

Ω – rotary (spindle) speed (rpm)

f – Feed rate (mm/min)

D – Duameter (mm)

Input parameters considered are –

h_0 = 0.2 mm, 0.3 mm, 0.4 mm

Ω – 1000 rpm, 1500 rpm, 2000 rpm

f – 30 mm/min, 35 mm/min, 40 mm/min

D – 36.50mm, 35.00mm, 33.50mm

Experiment has used three combinations in each level for input parameters, which has been tabulated below :

Table 2: Experimental data depicting material removal rate for the Phase-1 experiment

Phase 1					
Experiment No.		h_0 (mm)	Ω (rpm)	f (mm/min)	MMR-
Experiment combination 1	C1	0.2	1000	30	20
	C2	0.2	1000	35	23
	C3	0.2	1000	40	29
Experiment Combination 2	C4	0.2	1500	30	20
	C5	0.2	1500	35	25
	C6	0.2	1500	40	29
Experiment Combination 3	C7	0.2	2000	30	20
	C8	0.2	2000	35	25

	C9	0.2	2000	40	29

Table 3: Experimental data depicting material removal rate for the Phase-2 experiment

Phase 2					
Experiment No.		**h_0 (mm)**	**Ω (rpm)**	**f (mm/min)**	**MMR-**
Experiment combination 1	C10	0.3	1000	30	30
	C11	0.3	1000	35	35
	C12	0.3	1000	40	40
Experiment Combination 2	C13	0.3	1500	30	32
	C14	0.3	1500	35	38
	C15	0.3	1500	40	40
Experiment Combination 3	C16	0.3	2000	30	32
	C17	0.3	2000	35	38
	C18	0.3	2000	40	43

Table 4: Experimental data depicting material removal rate for the Phase-3 experiment

Phase 3					
Experiment No.		**h_0 (mm)**	**Ω (rpm)**	**f (mm/min)**	**MMR-**
Experiment combination 1	C19	0.4	1000	30	43
	C20	0.4	1000	35	48
	C21	0.4	1000	40	57
Experiment Combination 2	C22	0.4	1500	30	40
	C23	0.4	1500	35	47
	C24	0.4	1500	40	48
Experiment Combination 3	C25	0.4	2000	30	43
	C26	0.4	2000	35	56
	C27	0.4	2000	40	56

Since experiment has been scheduled to record vibration or noise generated during turning process or to record chatter of the turning experiment high quality microphone has been fitted at appropriate distance of cutting tool and workpice interference. Special attention has been paid during placing the microphone that no subsidery noise or object should come in contact with the microphone. For sound recording sensitive software has been used. The microphone has been connected to the laptop where inut sound of chatter has been filtered and recorded.

Stability lobe diagram (SLD)

The dept of cut or chip width (b) is most significant cutting paramaeter in deciding the generation of chatter in a turning process. The tool chatter issue has been attempted to be expressed by earlier academics using more complex models. Last but not least, they believed

that a single degree second order delay differential equation was adequate to accurately capture the tool chatter phenomenon. Higher order terms are unnecessary, and they produced incorrect and unnecessary solutions[32],[33]. It has been determined, after analyzing a number of models based on multiple degrees of freedom, that the two degrees of freedom model is superfluous and that the analysis can be done quickly and accurately by taking into account the single degree of freedom system[34]. Additionally, a system with a single degree of freedom is able to predict chatter during the turning process with accuracy. To access the set of spindle speed and depth of cut relating to steady turning, SLD has been drawn. SLD is very handy in prediction of chatter stability in turning process and it makes easy to choose ideal spindle speed and depth of cut combinations for maximum MRR in a turning process. The following is a presentation of the thorough mathematical study used to determine the stability lobes. Figure 2 illustrates the delay mechanism between the subsequent turning passes.

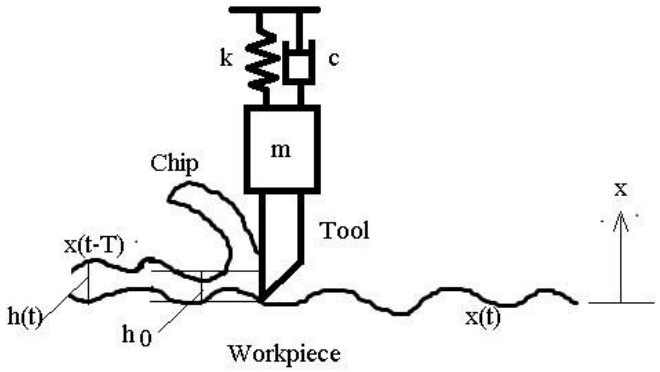

Figure 2: Delay between the consecutive turning passes

The equation of motion for single-degree of freedom (sDoF) system of mass (m), spring constant (k) and damping coefficient (c) excited by a non-linear cutting force (F(t)) is represented by [35], [36]. Using a non-linear cutting force (F(t)), the equation of motion for a single-degree of freedom (sDoF) system with mass (m), spring constant (k), and damping coefficient (c) is shown in [9], [10] following equation -

$$m\frac{d^2x(t)}{dt^2}+c\frac{dx(t)}{dt}+k\,x(t)=F(t) \qquad \text{.....eq18}$$

Now dividing equation 18 by 'm' and substituting natural frequency $\omega_n=\sqrt{k/m}$ and damping ratio of the system $\zeta=c/2\sqrt{km}$, following equation has been obtained -

$$\frac{d^2x(t)}{dt^2}+2\zeta\omega_n\frac{dx(t)}{dt}+\omega_n^2x(t)=\frac{\omega_n^2}{k}F(t) \qquad \text{.....eq19}$$

Initially, the workpiece's surface is smooth during the turning operation's first revolution, but as a result of chatter vibrations of the workpiece, the tool begins to leave a wavy surface behind. When the second revolution begins, there are waves on the surface on both sides: inside the cut where the tool is cutting (i.e., inner modulation, x(t)), and on the exterior surface of the cut due to vibrations during the previous revolution of cut (i.e., outer modulation, x(t-

T)). Thus, the dynamic chip thickness that results is no longer constant. Consequently, the dynamics equation for a linear mass-spring-damper system with sDoF activated by a nonlinear cutting force is as follows -

$$m\frac{d^2x(t)}{dt^2}+c\frac{dx(t)}{dt}+k\,x(t)=F_f(t)=K_f ah(t) \quad \text{.....eq}$$

$$\frac{d^2x(t)}{dt^2}+2\zeta\omega_n\frac{dx(t)}{dt}+\omega_n^2x(t)=\frac{\omega_n^2}{k}K_f a[h_0+x(t-T)-x(t)] \quad \text{.....eq21}$$

In the equation 21,

the static chip thickness is denoted by (h_0)

the dynamic chip thickness is denoted by (x(t - T)- x(t))

the delay time denoted by "T", which indicates the dependency of tool on earlier position.

Let's assume,

$$\tau=\omega_n t,\delta=\omega_n T,d\tau=\omega_n dt,\frac{d\tau}{dt}=\omega_n \quad \text{.....eq 22}$$

$$\frac{dx(t)}{dt}=\frac{dx(t)}{d\tau}\frac{d\tau}{dt}=\frac{dx(t)}{d\tau}\omega_n$$

and

$$\frac{d^2x(t)}{dt^2}=\frac{d}{dt}\left(\frac{dx(t)}{d\tau}\omega_n\right)=\frac{d^2x(t)}{d\tau^2}\omega_n^2 \quad \text{..... eq23}$$

If we substituting the values of equation 22 and equation 23 in equation 21 for (h0 = 0), following equation is derived -

$$\omega_n^2\frac{d^2x(\tau)}{d\tau^2}+2\zeta\omega_n^2\frac{dx(\tau)}{d\tau}+\omega_n^2x(\tau)=\frac{\omega_n^2}{k}K_f a[x(\tau-\delta)-x(\tau)] \quad \text{.....eq24}$$

$$\frac{d^2x(\tau)}{d\tau^2}+2\zeta\frac{dx(\tau)}{d\tau}+[1+w]x(\tau)=w[x(\tau-\delta)] \quad \text{.....eq25}$$

Where $w=K_f a/k$

Applying Laplace transform to the equation 25

$$s^2x(s)+2\zeta sx(s)+[1+w]x(s)=we^{-\delta s}x(s)$$

$$s^2+2\zeta s+[1+w]-we^{-\delta s} \quad \text{.....eq26}$$

Now

- equate the roots of specific equation 26, equal to 0, for critical stable limits.
- and substituting $s=ir_\omega$, where

$$r_\omega = \omega_c / \omega_n$$

$$\text{and } e^{-i\delta r_\omega} = \cos\delta r_\omega - i\sin\delta r_\omega$$

The resulting equation obtained is -

$$\ldots\ldots \text{eq}2' -r_\omega^{\,2} + i2\zeta r_\omega + [1+w] - w\cos\delta r_\omega - iw\sin\delta r_\omega = 0$$

If real part = $1 - r_\omega^{\,2} + w = w\cos\delta r_\omega$ and imaginary part = $2\zeta r_\omega = -w\sin\delta r_\omega$. Therefore,

$$w = -\frac{\left(1-r_\omega^{\,2}\right)^2 + \left(2\zeta r_\omega\right)^2}{2(1-r_\omega^{\,2})} \qquad \ldots\ldots\ldots \text{eq}28$$

The physical depth of cut on the stability lobes are denoted by $w = K_f a / k$

Therefore 'a' becomes

$$a = \frac{k}{K_f}\frac{\left(1-r_\omega^{\,2}\right)^2 + \left(2\zeta r_\omega\right)^2}{2(1-r_\omega^{\,2})} \qquad \ldots\ldots\ldots \text{eq}29$$

Now substituting thevalue

$$\sin\delta r_\omega = 2\tan\frac{\delta r_\omega}{2} \Big/ \left[1 + \tan^2\left(\frac{\delta r_\omega}{2}\right)\right]$$

into the imaginary part $2\zeta r_\omega = -w\sin\delta r_\omega$ and

substituting the value

$$\cos\delta r_\omega = \frac{1 - \tan^2\left(\frac{\delta r_\omega}{2}\right)}{1 + \tan^2\left(\frac{\delta r_\omega}{2}\right)}$$

into the real part $1 - r_\omega^{\,2} + w = w\cos\delta r_\omega$

the equation 27 produce the following equation as a result -

$$w = -\frac{2\zeta r_\omega}{\sin\delta r_\omega} = -\frac{1+\tan^2\left(\frac{\delta r_\omega}{2}\right)}{\tan\frac{\delta r_\omega}{2}}\zeta r_\omega \;\; and \;\; \delta = \frac{2}{r_\omega}\left[\tan^{-1}\left(\frac{1-r_\omega^{\,2}}{2\zeta r_\omega}\right) + n_l\pi\right] \qquad \ldots\ldots\ldots \text{eq } 30$$

In the euation 30

n_1 - the integer number that indicates the number of the lobes,

this integer number represents the border between the unstable and the stable area of the stability chart;

$$\delta = \frac{2}{r_\omega}\left[\psi + \frac{2n_l - 1}{2}\pi\right] \quad Where, \psi = \tan^{-1}\frac{-2\zeta r_\omega}{1 - r_\omega^{\,2}} \qquad \text{……..eq31}$$

Time dely (T) obtained from the equation 22 and equation 31 produced as

$$T = \frac{\delta}{\omega_n} = \frac{2}{\omega_n r_\omega}\left[\tan^{-1}\left(\frac{1 - r_\omega^{\,2}}{2\zeta r_\omega}\right)\right] + n_l\pi = \frac{2}{\omega_n r_\omega}\left[\psi + \frac{2n_l - 1}{2}\pi\right]$$

$$\frac{2\pi n[rev/s]}{\omega_n} = \frac{2\pi}{\delta} = \frac{2\pi r_\omega}{2\left[\tan^{-1}\left(\frac{1 - r_\omega^{\,2}}{2\zeta r_\omega}\right) + n_l\pi\right]} = \frac{2\pi r_\omega}{2\left[\psi + \frac{2n_l - 1}{2}\pi\right]}$$

Spindle speed produced as -

$$n[rev/s] = \frac{r_\omega \omega_n}{2\left[\tan^{-1}\left(\frac{1 - r_\omega^{\,2}}{2\zeta r_\omega}\right) + n_l\pi\right]} = \frac{r_\omega \omega_n}{2\left[\psi + \frac{2n_l - 1}{2}\pi\right]}$$

……eq32

Regenerative phase is produced as

$$\varepsilon = \omega T = 2\left[\psi + \frac{2n_l - 1}{2}\pi\right] = 2\psi + (2n_l - 1)\pi \qquad \text{……..eq33}$$

The stability lobes can be derived at excitation ratio $r_\omega = \omega_c / \omega_n = \sqrt{1 + 2\zeta}$,

Since $\zeta \approx 0$, i.e. the value is very less for orthogonal cutting, therefor, the critical depth of cut is represented by

$$a_{cr} = 2k\zeta(1 + \zeta)/K_f \approx 2k\zeta/K_f \qquad \text{…….eq34}$$

For minimum depth of cut, the Spindle speed is obtained as –

$$n[rev/s] = \frac{r_\omega \omega_n}{2\left[\tan^{-1}\left(\frac{1 - 1 - 2\zeta}{2\zeta\sqrt{1 + 2\zeta}}\right) + n_l\pi\right]} \approx \frac{\omega_n}{2\left[\frac{-\pi}{4} + n_l\pi\right]} = \frac{\omega_n}{2\pi}\frac{4}{4n_l - 1}$$

……..eq35

For the aforementioned equation, the stability lobe diagram is obtained by plotting the stability limits and chatter frequency. Some of the observed system's dynamic properties must be known in order to build the stability lobe diagram. The machine tool-tool holder-tool system's Transfer Function (TF) or Frequency Response Function (FRF) provides the system with the necessary information (dynamic properties). In the current study, an impulse hammer is used to stimulate

the tool, and a vibration acquisition sensor was used to track its reaction. The natural frequency, modal stiffness, and damping coefficient of the tool vibration, which are typically obtained by the frequency response function (FRF) of the system, must be calculated in order to create the stability lobe diagram of the tool vibration.

Utilizing an impulse excitation force, an experimental identification of the frequency response function of the observed cutting tool was made. The Al6061-T6 workpiece was turned in the current project using an MTAB XL-TURN CNC lathe with a Carbide insert TTS04. Using an impact hammer to excite the tool, the excitation signals are transmitted to the PC via an AID converter where they are tabulated and stored. A microphone is used to capture the auditory signals associated with tool vibration, and these signals are also tabulated and stored. The obtained time domain signals are then subjected to a Fast Fourier Transformation (FFT) using MATLAB software. These FFT signals were used to calculate the system's FRF, or its real and imaginary components. To detennine the modal parameters (k, c and Kf) for generating the stability lobe diagrams obtained FRF's have been used and the Figure 3 illistrate the stability lobes diagram ploted

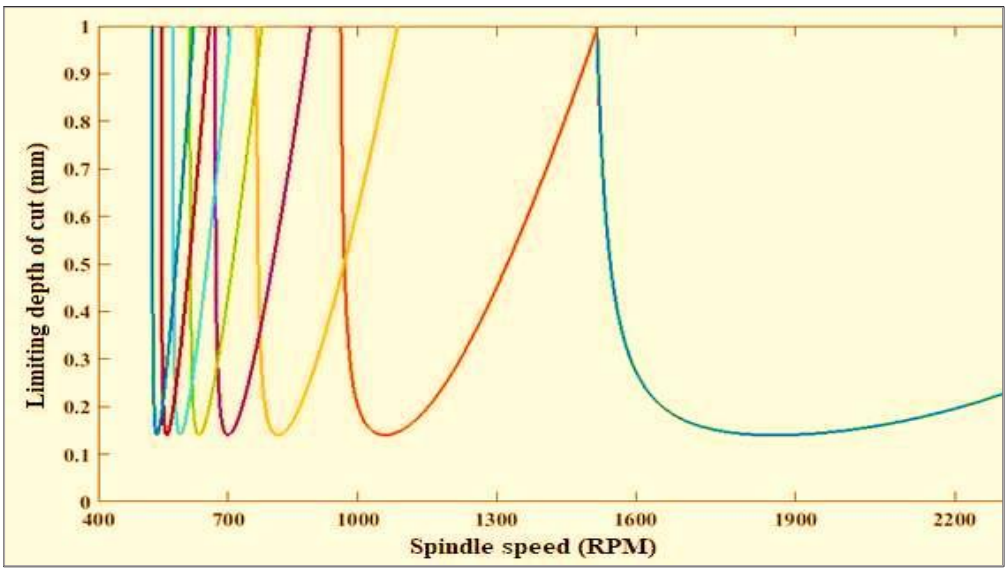

Figure 3: Stability lobe diagram as per obtained FRS's

The boundary between stable and unstable machining in terms of different combination of cutting depth and spinning speeds is represented by the stability lobe diagramSLD. It's a safe area or region with very low chatter under the lobes. Conversely, the region beyond the lobes is in a fragile state. Therefore, selection of a combination of input parametersspindle speed and cut depth within the safe zone is recommended.

The main objective of contemporary industries is to produce goods of exceptional quality while increasing productivity since demand and supply has got paramount importance in the age of science and technology. Turning operation is one of the most expected industries where improvement is eminent and the productivity in turning operations is correlated with material removal rate (MRR). Achieving a higher material removal rate can boost the productivity of certain manufacturing sectors. The input process parameters, such as feed rate, spindle speed, and depth of cut, directly affect MRR. Since industries and consumers demands for high quality product with high rate of accuracy and finishing is increasing, turning process has to take acoount of the chatter to suppress the roughness of product. Since higher the affecting numbers, the greater the rate of material removal and, thus, the greater the productivity. Chatter, on the other hand, depends on the input turning parameters non-monotonically. Additionally, chatter is a natural occurrence that cannot be entirely stopped. However, it can be prevented by selecting the right set of turning settings.

The selection of an appropriate range of turning parameters is therefore crucial for increased MRR while minimizing chatter. Only after determining how closely outputs (chatter severity and MRR) relate on input turning parameters can this be accomplished. By creating output prediction models using Response Surface Methodology (RSM) and Artificial Neural Network (ANN) techniques, the chapter's goal was realized. Additionally, a comparison of the mathematical models produced by RSM and ANN has been conducted in order to determine which the most suitable one was.

Experimental output analysis

Manufacturing sectors' top priority is to increase productivity by reducing production costs in the current competitive environment. This can only be accomplished by manufacturing items with high tolerance and good surface quality at a faster rate of material removal. In turning operation chatter is considerd to important factor that need attention. Tool chatter is a problem that restricts how quickly materials are removed in many industries. To produce superior products at a higher rate of material removal, a suitable range of machining parameters must be chosen. In this experiment we have focused on material removal rate which is essential for the fast product lienup, chatter feature extraction, essential for surface roughness suppression.

Analysis of Material removal rate (MRR)

The workpiece's surface quality and material removal rate are primarily responsible for the greater production rate. Surface quality and MRR should be good in order to produce a product of the highest quality and profit. Experimental data obtained shows different rate of material removal rate at differnet spindle speed Ω (rpm) and feed rate with different depth of cut. Tables 5, 6, and 7 summerise the data obtained from experiment with calculated values for material removal rate for different combinations applied. Calculated data indicate increase in spindle speed increases material removal rate.

Table 5: Experimental data depicting material removal rate for the Phase-1 experiment

Phase 1					
Experiment No.		**h_0 (mm)**	**Ω (rpm)**	**f (mm/min)**	**MMR-**
Experiment combination 1	C1	0.2	1000	30	20
	C2	0.2	1000	35	23
	C3	0.2	1000	40	29
Experiment Combination 2	C4	0.2	1500	30	20
	C5	0.2	1500	35	25
	C6	0.2	1500	40	29
Experiment Combination 3	C7	0.2	2000	30	20
	C8	0.2	2000	35	25
	C9	0.2	2000	40	29

Table 6: Experimental data depicting material removal rate for the Phase-2 experiment

Phase 2					
Experiment No.		**h_0 (mm)**	**Ω (rpm)**	**f (mm/min)**	**MMR-**
Experiment combination 1	C10	0.3	1000	30	30
	C11	0.3	1000	35	35
	C12	0.3	1000	40	40
Experiment Combination 2	C13	0.3	1500	30	32
	C14	0.3	1500	35	38
	C15	0.3	1500	40	40
Experiment Combination 3	C16	0.3	2000	30	32
	C17	0.3	2000	35	38
	C18	0.3	2000	40	43

Table 7: Experimental data depicting material removal rate for the Phase-3 experiment

Phase 3					
Experiment No.		**h_0 (mm)**	**Ω (rpm)**	**f (mm/min)**	**MMR-**
Experiment combination 1	C19	0.4	1000	30	43
	C20	0.4	1000	35	48
	C21	0.4	1000	40	57
Experiment Combination 2	C22	0.4	1500	30	40
	C23	0.4	1500	35	47
	C24	0.4	1500	40	48
	C25	0.4	2000	30	43

Experiment Combination 3	C26	0.4	2000	35	56
	C27	0.4	2000	40	56

Extraction of Chatter feature

Popular PFs responsible for chatter have been assessed using statistical chatter indicators in order to extract the chatter features. Three statistical chatter indicators were taken into account in this experiment to extract chatter features. In chatter extraction each signal is important in its own right hence significance of the statistical chatter indicators, value of root-mean-square value, peak to peak value and absolute mean amplitude has been analysed and discussed.

Value of the root-mean-square: The root mean square (RMS) is a metric for signal energy. The RMS value is the total of each individual RMS value when the noise from two different sources is added. Stronger RMS values signify a stronger chatter component in a signal in physical mode and its value is the square root of the mean square of the signal amplitudes measured over a period of time. The equation 50 has been applied to determine RMS value.

$$x_{rms}(t) = \sqrt{\frac{1}{N}\sum_{n=1}^{N} x(t)^2}$$

……eq50

In the equation 50, x (t) is the signal, and N is the length of the signal.

Peak to peak value: The measurement from crest to trough of a signal is called peak to peak value i.e. the difference between positive peak and neagative peak. The chatter will be more intense the higher peak-to-peak value. The formula has been used to determine the peak to peak value;

$$X(t)_p = \max(x(t)) — \min(x(t))$$ ……...eq51

Absolute mean amplitude (AMA): The average of the absolute values of chatter amplitudes is known as the absolute mean amplitude (AMA). Because the cutting force fluctuates, the recorded signals can have positive or negative amplitudes. The absolute mean amplitude is thus obtained by averaging the absolute values of all the recorded signals. The signal's buzz components will be greater the higher the AMA value. Equation 52 have been used for the calculation of AMA.

$$\frac{1}{N}\sum_{n=1}^{N} |x(t)|$$

…….eq52

In equation 52 x(t) is the signal and N is the length of the signal.

Researchers have determined that spindle speed and depth of cut have the greatest influence on chatter during turning. However, the effect of feed rate on chatter has also been examined in the current study, which was not done by the earlier researchers. Cutting parameter values have been altered, and turning tests have been carried out using various combinations of cutting parameters in an effort to identify the chatter phenomena. Then, notable product functions (PFs) have been chosen for the matching experimental combination signals. the developed statistical chatter indicators for these combinations have been summurised in Tables below.

Table 8: Standard chatter indicators (PFs) for Pahse-1 experiment

Phase 1							
Experiment No.		**h_0 (mm)**	**Ω (rpm)**	**f (mm/min)**	**RMS**	**P-to-P**	**AMA**
ExpC1	C1	0.2	1000	30	2.4	29.2	1.99
	C2	0.2	1000	35	2.3	29.6	1.76
	C3	0.2	1000	40	1.6	22.7	1.42
ExpC2	C4	0.2	1500	30	3.6	47.9	2.73
	C5	0.2	1500	35	2.5	25.1	1.85
	C6	0.2	1500	40	2.5	24.5	1.87
ExpC3	C7	0.2	2000	30	3.6	35.6	3.67
	C8	0.2	2000	35	4.1	40.9	3.07
	C9	0.2	2000	40	4.5	46.8	3.38

Table 9: Standard chatter indicators (PFs) for Pahse-2 experiment

Phase 2							
Experiment No.		**h_0 (mm)**	**Ω (rpm)**	**f (mm/min)**	**RMS**	**P-to-P**	**AMA**
ExpC1	C10	0.3	1000	30	1.5	22.7	1.10
	C11	0.3	1000	35	2.3	34.6	1.03
	C12	0.3	1000	40	1.6	18.2	1.22
ExpC2	C13	0.3	1500	30	2.6	27.1	1.97
	C14	0.3	1500	35	1.8	15.5	1.40
	C15	0.3	1500	40	1.8	17.2	1.79
ExpC3	C16	0.3	2000	30	4.7	41.8	3.48
	C17	0.3	2000	35	4.7	44.0	3.48
	C18	0.3	2000	40	4.9	43.2	3.72

Table 10: Standard chatter indicators (PFs) for Pahse-2 experiment

Phase 3							
Experiment No.		**h_0 (mm)**	**Ω (rpm)**	**f (mm/min)**	**RMS**	**P-to-P**	**AMA**
ExpC1	C19	0.4	1000	30	2.5	29.9	1.89
	C20	0.4	1000	35	2.4	32.5	1.77
	C21	0.4	1000	40	1.8	23.2	1.92
ExpC2	C22	0.4	1500	30	3.1	38.8	2.34
	C23	0.4	1500	35	3.2	26.5	2.43
	C24	0.4	1500	40	3.1	30.5	2.34
ExpC3	C25	0.4	2000	30	4.1	45.5	3.11
	C26	0.4	2000	35	4.0	39.5	3.02
	C27	0.4	2000	40	4.7	44.1	3.55

Chatter is an inevitable feature in turning operations, as it has been discussed in previous chapters and have been already established. Nevertheless, it can be prevented by selecting the right input turning parameters as theoretically and logicaly suggested by various cholars in this direction also. Therefore, it is crucial to extract the tool chatter's features. Chatter or vibration characteristics in this context refer to the volume and intensity of vibratio or chatter. As per the chatter characterisitics three types of chatter can be distinguished: stable, moderate (a transition between stable and unstable), and unstable. Chatter characteristics can be determined by examining the statistical data obtained in the experiment as summurised in Tables 8,9,10. It is crucial to determine an appropriate chatter threshold value in order to classify the type of chatter. In order to find the values of chatter thresolds for the three statistical chatter indicators, Nakagami distribution approach has been applied.

Threshold analysis with Nakagami distribution

A probability distribution method called the Nakagami distribution is used to simulate scattered signals [37] or to model scattered signals that reach a receiver by multiple paths, where depending on the density of the scatter, the signal will display differnet fading characteristics. It is a general method to describe small scale fading for dense signal scatters, depending on the scatter's density. Because the signal exhibits various fading characteristics, the amount of fading is more in control with this distribution. The shape parameter and the spread parameter are its two parameters used in Nakagami distribution. With the shape parameter set to $p > 0.5$ and the spread parameter set to $\omega > 0$, for all random variables $x > 0$, these two parameters are used to ascertain the height, steepness, and concavity of the probability density curve. Exponential decrease of tail can be detected for the large value of x and for x less than or equal to zero the probability density function is zero. The Nakagami distribution's probability density function is given by;

$$PDF = \frac{2\mu^{\mu}}{\Gamma(\mu)\omega^{\mu}} x^{(2\mu-1)} e^{(-\frac{\mu}{\omega}x^2)}$$

…….. eq 53

Equation 53 can be explained as, shape parameter μ and scale parameter ω > 0, for x > 0. If x has a Nakagami distribution with parameters μ and ω, then x^2 has a gamma distribution with scale parameter ω/μ and shape parameter μ. Probability density functions for root mean square value, peak-to-peak value and absolute mean amplitude, the three statistical indicators, have been calculated and graphs ploted as shown in figures 49 a, b and c. After that, threshold limits were determined using the Nakagami technique, where the upper and lower limits were established using m±σ, where m indicate mean and σ indicate standard deviation of probability distribution function values. Green and red lines in Fig. 49, respectively, represent the lower and upper threshold limits. The statistical indicator values between the green and red lines reflect mild chatter, the values on the right side of the red line represent unstable chatter, and the values on the left side of the green line represent steady machining.

In order to visualize the variation in the statistical chatter indicator with respect to the experiment combinations of cutting parameters, statistical chatter indicators, as shown in Table 8,9,10 for all phases, were displayed after the threshold values were established. The plot between the statistical chatter indicators and experimental runs has been illustrated in Figures 4(d), (e), and (f) where below the green threshold line, stable turning has been observed. Experimental runs that fall outside red threshold line in the graph indicates erratic turning where extreme chatter has been observed, while in between the green and red threshold lines moderate experimental turning or transition turning has been observed. Experimental values obtained have been plotted on stability lobe diagrams to verify the nature of chatter for all phses and combinations.

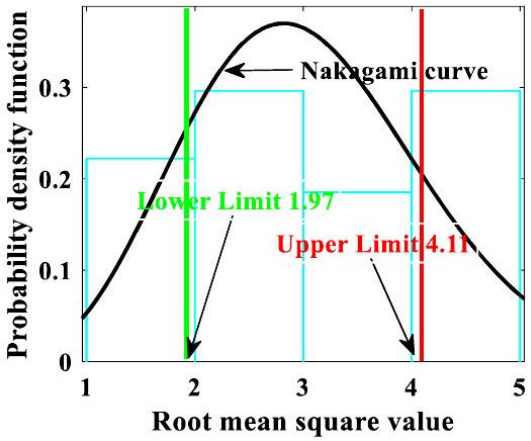

(a – PDF vs RMS value)

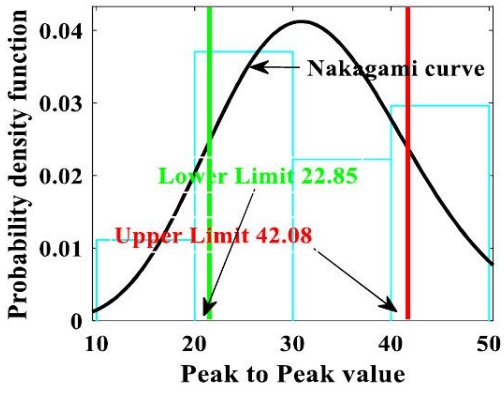

(b – PDF vs P-to-P value)

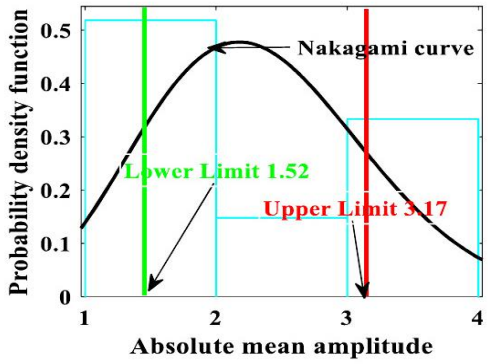

(c – PDF vs AMA value)

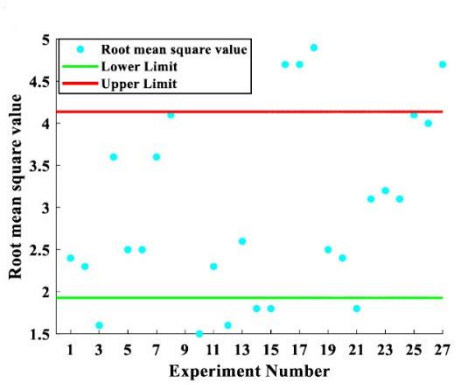

(d – RMS Value vs Experimental numbers)

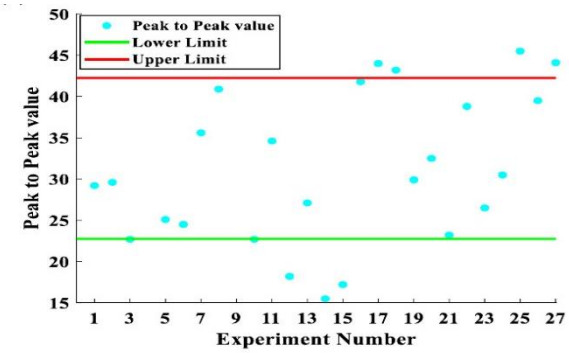

(e – P-to-P value vs Experimental numbers)

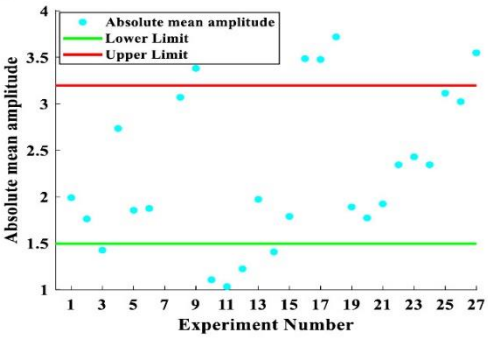

(f – AMA Value vs Experimental numbers)

Figures 4: Threshold ananlysis

Plotting Stability lobe diagram

The two-dimensional graphic known as the stability lobe diagram (SLD) is useful for figuring out the turning stability. SLD, which takes the shape of diverse combinations of depth of cut and spindle speed, represents the boundary between stable and unstable machining. Stable machining occurs in the area below the SLD curves, whereas unstable machining occurs in the area above the SLD curves. The cutting force between the tool and the workpiece increases as the depth of cut increases, causing chatter to become more pronounced and the point to intersect the SLD curve. The presence of chatter is indicated by the appearance of anomalous frequency components at this time, and the associated frequency is referred to as the chatter frequency. Some experiment values are discovered to sit on the SLD plot's boundary when the various turning combinations are plotted on the SLD. These are the points of transition. The primary flaw with stability lobe is that it is unable to foresee how feed rate will affect chatter.

Figures 4(d), (e), and (f) have been statistically analyzed where feed rate, spindle speed, and depth of cut has been taken into account for ascertaining the impact on turning experiment. Using the stability lobe diagram presented in Figure 5, the statistical predictions have been cross-checked. The experiment no. 7 of phse 3 has been labeled risky as per AMA data observed, while the same experiment has been labeled safe by the other two statistical indicators, according to an analysis of all the statistical chatter indicators in Figures 4.

Additionally, the AMA gave the experiments 6 of phase 1 and experiment 4 of phase 2 a moderate rating. However, other two statistical indicators have deemed these experiments to be risky. Additionally, the stability lobe diagram matches up well with the stability criterion proposed by AMA. Therefore, it has been concluded that the absolute mean amplitude (AMA) more clearly illustrates the chatter behavior.

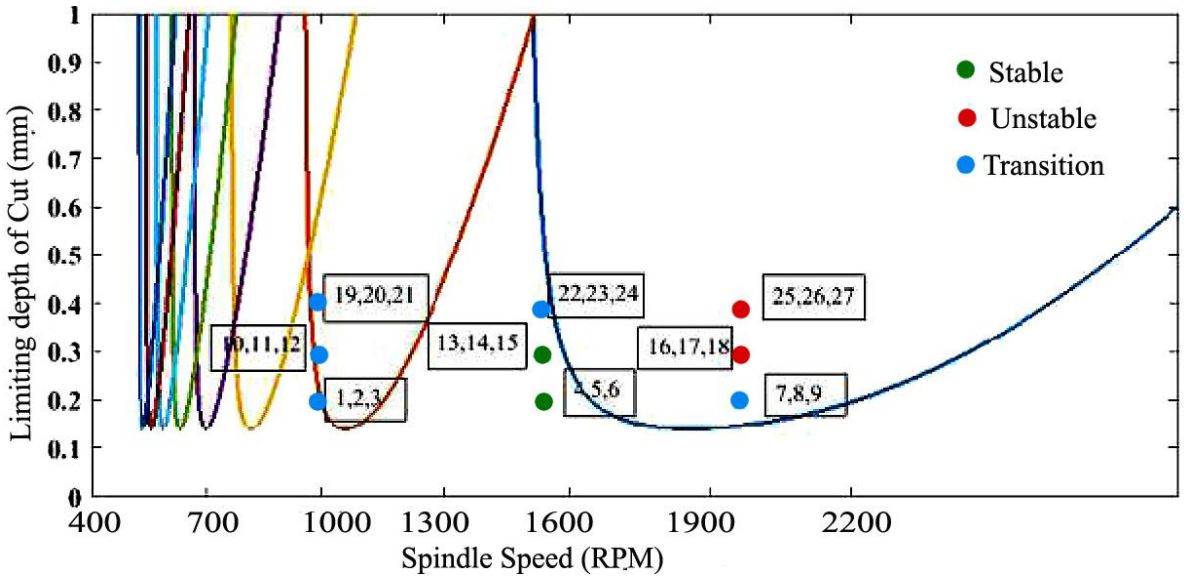

Figure 5: Stability lobe diagram on the basis of statistical data obtained

Additionally, it has been found from the research conducted by numerous researchers that, even though the chatter process may be managed by carefully choosing the cutting settings, there are occasions when it defies the controls and sharply grows. The inhomogeneous character of the work material is what causes the modulated chip thickness and dynamically affects the cutting force, which is why the trend is so unexpected. The system becomes unstable when the modulated cutting force frequency reaches the cutting system's native frequencies. AMA values resemble talk more visibly in the present, it may be seen. As a result, the more AMA is valued, the more talk there will be. Consequently to extract chatter features, AMA is a crucial output component that must be taken into account. The stability chart has been generated for the list of trials that have been marked as having stable, moderate, and unstable chatter, as given in Table 11, after a critical analysis of Figures 4(d), (e), and (f). It is clear from comparing these values to the position in the stability lobe diagram that AMA is the best statistical indication for predicting the type of chatter out of the three. Therefore, AMA has been chosen in subsequent analysis to ensure steady turning at enhanced MRR.

Table 11: Stability chart of Experiments

Statistical Indicator	Stable	Moderate	Unstable
RMS	2, 3,8,11,13,19	1,2,7,5,6,10,12,16,14,20,21,	4,9,15,17,18,27

		22,23,24,25,26	
Peak to Peak	3,10,12,14,15,21	1,2,4,5,6,7,8,11,13,19,20, 22,23,24,25,26	9,16,17,18,27
AMA	2,10,12,14,15,21	1,3,4,5,6,7,8,9,11,13,16, 19,20,22,23,24,26	17,18,25,27

The highest limit and lower limit of the AMA threshold values are 3.17 and 1.52, respectively. The likelihood of attaining steady machining is indicated if the AMA value is below the lower limit which has been observed in 1,4 and 5 in table 20 where the values are below lower limit i.e. 1.42,1.03 and 1.4 respectively. Here extraordinarily smooth surface topographies with hardly any chatter marks hs been observed. Similar to this, if AMA readings are beyond the upper threshold limit, there is a potential of unstable machining which has been observed in 3, 6 and 10 serials in table 6.4 where the values obaserved has been 3.38, 3.47 and 3.55. Here severe chatter marks have been observed with high roughness. As long as the AMA values of the related experiments are between the two extreme threshold values, mild chatter marks have been observed. It is simple to determine that the Nakagami distribution is appropriate for determining the likelihood of obtaining stable range of machining after studying these surface topographies. Analysis indicates that the developed threshold values using Nakagami approach are correct.

Table 20: Surface topography at different combinations of turning parameters

S. No.	h_0 (mm)	Ω (rpm)	f (mm/min)	AMA	Roughness
1	0.2	1000	40	1.42	smooth
2	0.2	1500	30	2.73	Moderate
3	0.2	2000	40	3.38	Rough
4	0.3	1000	35	1.03	Smooth
5	0.3	1500	35	1.4	Smooth
6	0.3	2000	35	3.47	Rough
7	0.4	1000	35	1.77	Moderate
8	0.4	1000	40	1.92	Moderate
9	0.4	1500	30	2.34	Moderate

10	0.4	2000	40	3.55	Rough

Conclusion

The Paper envisase to find solution to improve the material removal rate without compromising the surface fisnish and machining tolerance of the workpiece, which compeled to consider the prediction model of MRR and chatter severity. These two factors have been developed and analysed to obtain optimal stablerange of turning parameters with lower chatter and improved material removal rate so that quality and accuracy could be mainained with high productivity. In predicting the stable zone for the optimal stable cutting and maximize material removal rate, stability lobe diagram has high probability of accuracy prediction.

Reference

1. Steven Y. Liang • Albert J. Shih Analysis of Machining and Machine Tools, ISBN 978-1-4899-7643-7 ISBN 978-1-4899-7645-1, Springer 2016
2. S.A. Tobias, Machine tool vibration research, International Journal of Machine Tool Design and Research 1 (1961) 1–14.
3. M. Wiercigroch, E. Budak, Sources of nonlinearities, chatter generation and suppression in metal cutting, philosophical transactions: Mathematical, Physical and Engineering Sciences 359 (2001) 663–693.
4. R.P.H. Faassen, Chatter prediction and control for high-speed milling: modelling and experiments, Technische Universiteit Eindhoven; Thesis (2007).
5. M. Wiercigroch, A.M. Krivtsov, Frictional chatter in orthogonal metal cutting, Philosophical Transactions: Mathematical, Physical and Engineer- ing Sciences (Series A) 359 (1781) (2001) 713–738.
6. M. Wiercigroch, E. Budak, Sources of nonlinearities, chatter generation and suppression in metal cutting, Philosophical Transactions of the Royal Society London 359 (2001) 663–693264.
7. S.A.Tobias, Machine Tools Vibrations (Vibracionesen Ma´ quinas-Herra-mientas), URMO, Spain, 1961.
8. J. Tlusty, M. Polacek, The stability of machine tools against self-excited vibrations in machining, International Research in Production Engineering (1963) 465–474.
9. J. Tlusty, Upper saddle river, Prentice-Hall, NJ, 2000.
10. M. Wiercigroch, E. Budak, Sources of nonlinearities, chatter generation and suppression in metal cutting, Philosophical Transactions of the Royal Society London 359 (2001) 663–693264.
11. L.R. Foulds, K. Neumann, A network flow model of group technology., Mathematical and Computer Modelling 38 (5-6) (2003/9) 623–635.

12. Y. Altintas, Manufacturing automation, metal cutting mechanics, Machine Tool Vibrations, and CNC Design, 2000, Cambridge University Press, USA, 2000.
13. R.P.H. Faassen, N. van de Wouw, J.A.J. Oosterling, H. Nijmeijer, Prediction of regenerative chatter by modelling and analysis of high-speed milling, International Journal of Machine Tools and Manufacture 43 (14) (2003/11) 1437–1446.
14. F. Taylor, on the art of cutting metals, Transactions of ASME 28 (1907).
15. R.N. Arnold, The mechanism of tool vibration in the cutting of steel, Proceedings of the Instituion of Mechanical Engineers 154 (1946) 261–284.
16. S.A. Tobias, W. Fishwick, The chatter of lathe tools under orthogonal cutting conditions, Transactions of ASME 80 (1958) 1079–1088.
17. J. Tlusty, M. Polacek, The stability of machine tools against self excited vibrations in machining, in: Proceedings of the International Research in Production Engineering Conference, Pittsburgh, PA, ASME, New York, 1963, pp. 465–474.
18. J. Tlusty, M. Polacek, The stability of machine tools against self excited vibrations in machining, in: Proceedings of the International Research in Production Engineering Conference, Pittsburgh, PA, ASME, New York, 1963, pp. 465–474.
19. S.A. Tobias, Machine Tool Vibration, Blackie and Sons Ltd, Glasglow, 1965.
20. H.E. Meritt, Theory of self-excited machine–tool chatter, Transactions of the ASME Journal of Engineering for Industry 87 (1965) 447–454.
21. Merritt, H. E. Theory of self-excited machine-tool chatter - Contribution to machine-tool chatter research – 1. ASME J. Eng. for Ind., 87, November 1965, 447-454.
22. Tlusty, J. Machine Dynamics. Handbook of High Speed Machining Technology. King, R. I., ed., 1985, Chapman and Hall, New York, Ch. 3, 48-153.
23. Tlusty, J. Dynamics of high-speed milling. J. of Engineering for Industry, Trans. ASME, 108, May 1986, 59-67.
24. Smith, S. & Tlusty, J. Update on high-speed milling dynamics. J. Engineering for Industry, Trans. ASME, 112, May 1990, 142-149.
25. K. Ahmadi and F. Ismail, "Analytical stability lobes including nonlinear process damping effect on machining chatter," International Journal of Machine Tools and Manufacture, vol. 51, no. 4, pp. 296-308, 2011.
26. M. Das and S. Tobias, "The relation between the static and the dynamic cutting of metals," International Journal of Machine Tool Design and Research, vol. 7, no. 2, pp. 63-89, 1967.
27. J. Tlusty, "Analysis of the state of research in cutting dynamics," Annals of the CIRP, vol. 27, no. 2, pp. 583-589, 1978.

28. Y. Yamane, T. Ryutaro, S. Tadanori, I. M. Ramirez, and Y. Keiji, "A new quantitative evaluation for characteristic of surface roughness in turning," Precision Engineering, 50, 2017, pp. 20-26.
29. M. Das and S. Tobias, "The relation between the static and the dynamic cutting of metals," International Journal of Machine Tool Design and Research, vol. 7, no. 2, pp. 63-89, 1967.
30. M. Siddhpura, A. Siddhpura, and R. Paurobally, "Chatter stability prediction for a flexible tool-workpiece system in a turning process," The International Journal of Advanced Manufacturing Technology, journal article pp. 1-16, 2017.
31. H. E. Merritt, "Theory of self-excited machine-tool chatter: contribution to machine-tool chatter research—," Journal of engineering for industry, vol. 87, no. 4, pp. 447¬454, 1965.
32. T. Insperger and G. Stépan, "Chatter suppression of turning process via periodic modulation of the spindle speed-a 1 DOF analysis," in Proceedings of 3rd Conference on Mechanical Engineering GEPESZET, 2002, pp. 720-724.
33. M. C. Salcedo, C. A. Pefialoza, and G. V. Ochoa, "Regenerative Reassembly Phenomenon in the Turning Process Machining the A1020 Steel," 2018.
34. N. Suzuki, K. Nishimura, E. Shamoto, K. J. J. 0. A. M. D. Yoshino, Systems, and Manufacturing, "Effect of cross transfer function on chatter stability in plunge cutting," vol. 4, no. 5, pp. 883-891, 2010.
35. Y. Altintas and M. Automation, "Metal cutting mechanics, machine tool vibrations, and CNC design," Manufacturing Automation, pp. 56-64, 2000.
36. Y. Altintas, G. Stepan, D. Merdol, and Z. Dombovari, "Chatter stability of milling in frequency and discrete time domain," CIRP Journal of Manufacturing Science and Technology, vol. 1, no. 1, pp. 35-44, 2008.
37. N. Nakagami, "The m-Distribution, a general formula of intensity of rapid fading In William C. Hoffman, editor, Statistical Methods in Radio Wave Propagation: Proc. Of a Symp. held June 18-20, 1958," ed: Permagon Press, 1960.